GAMMA FIELD IN WATER SURROUNDING A DUCT CONTAINING A SOURCE

by

Jack Clark Kaye

A Thesis Submitted to the
Graduate Faculty in Partial Fulfillment of
The Requirements for the Degree of
MASTER OF SCIENCE

Major Subject: Nuclear Engineering

Approved:

Signatures have been redacted for privacy

Iowa State University
Of Science and Technology
Ames, Iowa

1963

TABLE OF CONTENTS

INTRODUCTION

Radiation shielding requirements have imposed many problems on the nuclear field. Among these problems has been the determination or prediction of the effect of voids or air ducts on a gamma field. A number of related experiments have been conducted at Oak Ridge National Laboratory, Brookhaven National Laboratory, and the Nuclear Aerospace Research Facility. These have been directed toward verifying analytical methods for predicting the effects of ducts and voids.

This investigation was undertaken to measure the gamma field in water resulting from a Cobalt-60 source. The effect of a duct was investigated by measurements both in and out of the water medium. The measurements were made using the shield tank facility of Iowa State University's UTR-10 reactor. Associated with the tank facility was an instrument bridge for positioning detection equipment inside the tank.

The investigation provided the photon energy spectrum at each spatial point in addition to relative count rates and dose rates. The photon flux and energy spectrum specified the amount of radiation at each point. Integrated dose rates were determined in mr/hr.

REVIEW OF LITERATURE

A large amount of past literature concerning the effect of ducts or voids was classified when originally published. This material was gradually declassified or reissued as unclassified information. The Oak Ridge National Laboratory Core-Hole Facility and Bulk Shielding Facility together with the Brookhaven National Laboratory Lid-Tank Shielding Facility provided the bulk of early duct experiments. A description of these facilities is given by Goldstein (3).

Measurement of the effect of voids was made by Pratt and Kouts (7). Their investigation included both cylindrical and spherical voids of various sizes in a water medium. The detection equipment was placed outside the water medium with pile gammas serving as the source. The relative position of the duct to the source was held constant. Count rates were obtained for different detector positions and shield thicknesses by raising and lowering both the water level and detector.

More recent investigations include those of Collins (2) and Clark, et al., (1). Collins determined the dose rates above a water shield having a single duct. A 4hh-mc Cobalt-60 source was placed at one end of a 3-in. duct. Clark measured the gamma radiation streaming through a duct penetrating the wall of a shielded room. A 15.3-mc source was suspended in the center of the room. Dose rates due to radiation penetrating the duct were derived from measurements made outside the room.

These investigations were concerned with duct streaming and scattered gamma radiation outside the shielding medium. They were primarily undertaken to prove or disprove various theoretical techniques for estimating shield requirements.

EQUIPMENT

The shield tank facility of the UTR-10 provided the water medium for the investigation. This tank was 5 ft by 6 ft by 11½ ft high. An instrument bridge at the top of the facility and a ¼ in. diameter aluminum tube provided three-dimensional positioning of the detector. A plexiglass case protected the detector from water. Electrical leads were contained in a 20 ft pliable plastic tube. The instrument bridge, plastic case, and tube are shown in Figure 1.

The duct was an aluminum tube 3 in. in diameter, 9 ft long, and 57 mils thick. It was suspended by an inverted U shaped bracket attached to the duct with a ⅜-in. diameter pin. A rod, passed through the opening between the top of the tube and the rounded curve of the U, supported the duct. The pin through the top of the tube was perpendicular to the rod providing freedom of rotation about two axes. The two degrees of freedom allowed the duct to hang vertically. A cup was welded to the other end and filled with lead to provide negative buoyancy to the tube and to seal the submerged end. The method of suspending the duct is pictured in Figure 1.

A 1.15-mc Cobalt-60 source was used. The source was placed in the center of a paper cup and lowered into position in the middle of the duct. With the duct placed in the tank the source was positioned as shown in Figure 2.

A scintillation detector, Nuclear Chicago model 28-5, was used. The crystal was a thallium-activated sodium iodide cylinder 1 in. in

Figure 1. Detector, duct and instrument bridge

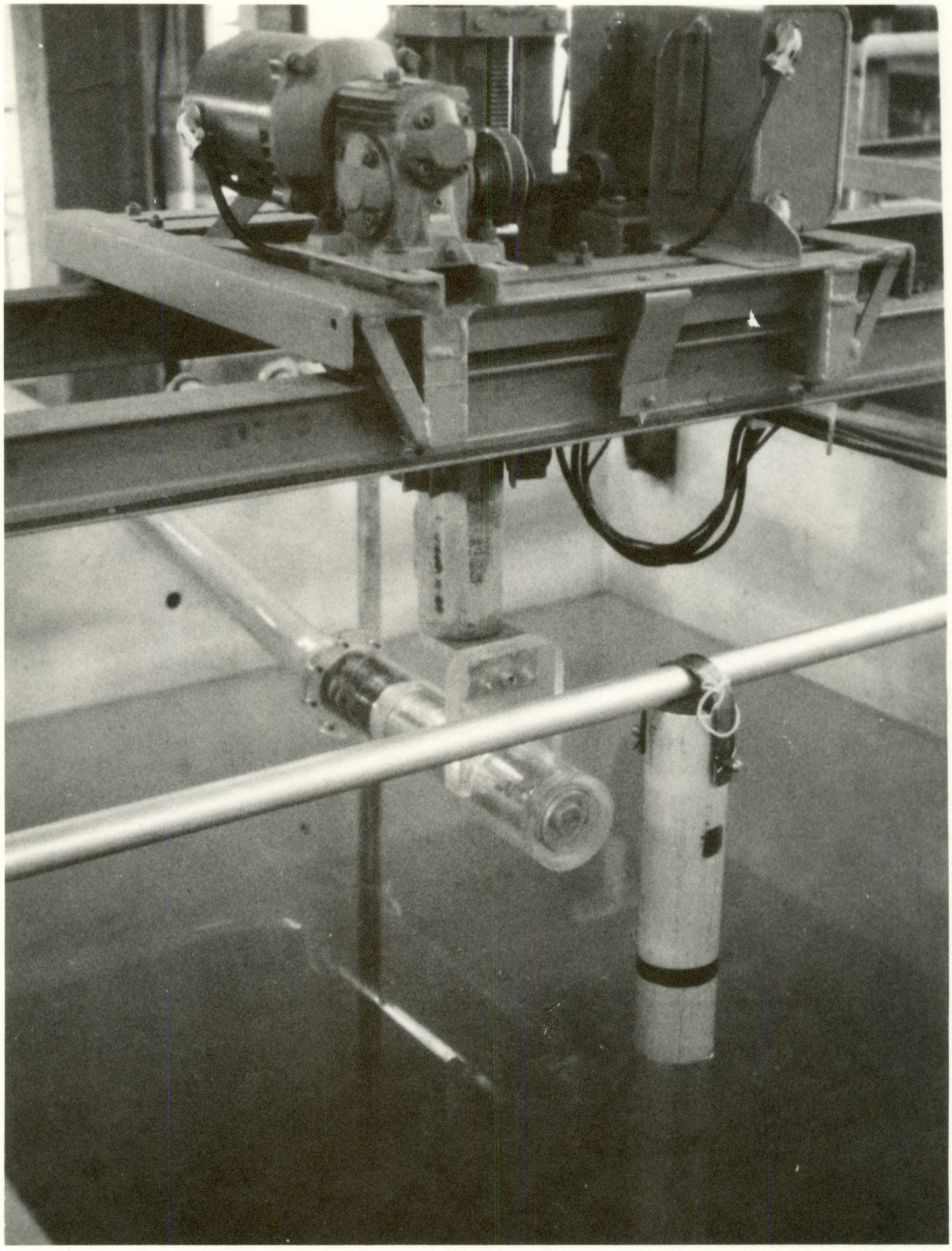

diameter by 1 in. long. A single channel, Nuclear Chicago radiation analyzer, model 1810, was used for measuring the energy spectrum. Counting was accomplished with a Nuclear Chicago ultrascaler model 192A-P. The resolving time of the first electronic decade of this scaler was 1 microsec. The maximum count rate was limited by the mechanical register to 170,000 cps.

Figure 2. Position of the source in the shield tank

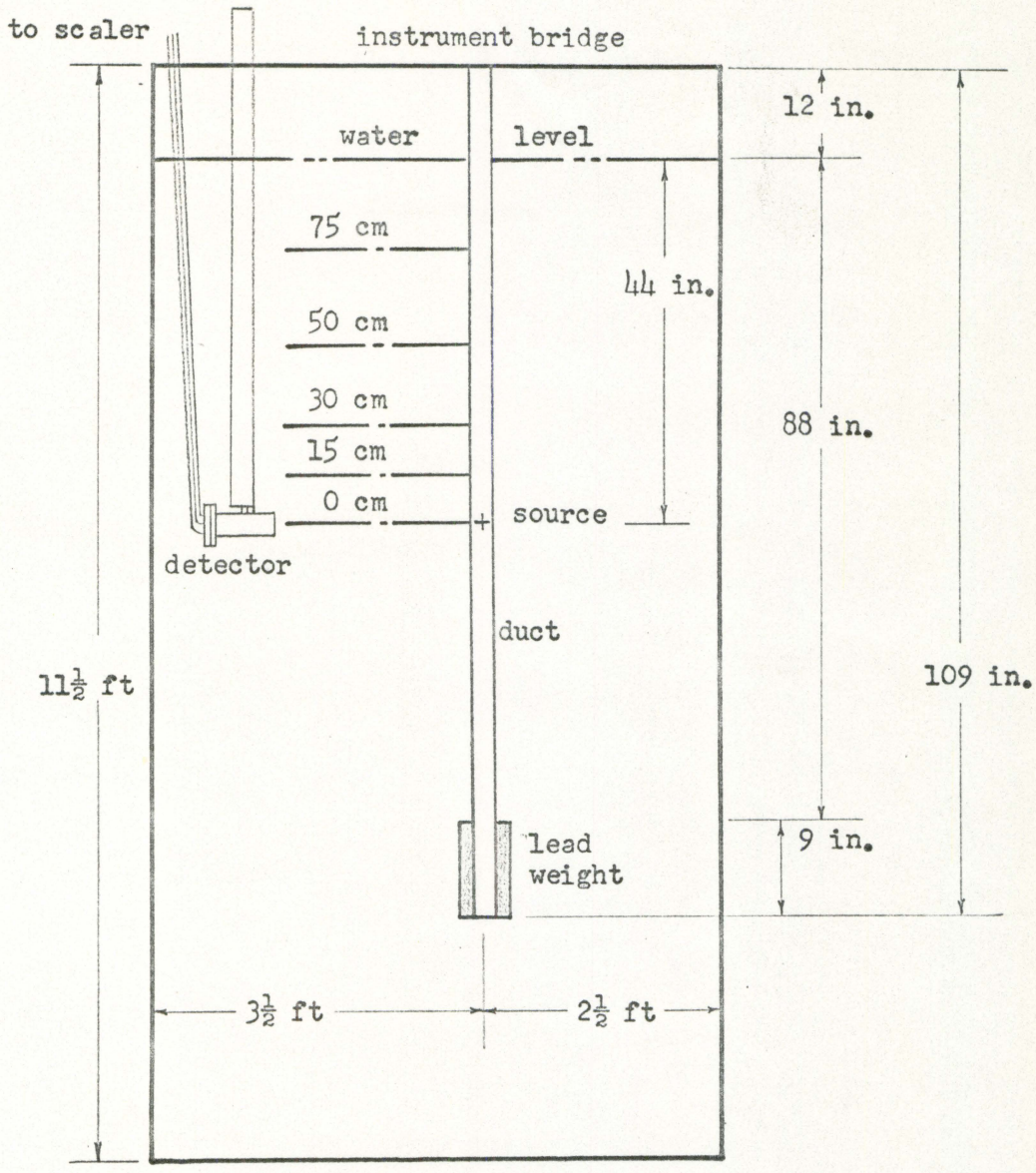
to scaler
instrument bridge
12 in.
water
level
75 cm
44 in.
50 cm
30 cm
88 in.
15 cm
0 cm
source
detector
duct
11½ ft
109 in.
lead
weight
9 in.
3½ ft
2½ ft

PROCEDURE

Prior to making the measurements pertinent to the investigation, the water tank was surveyed for background. The background radiation averaged about 100 cpm with energies less than 100 kev. The reactor had been idle for several hours prior to the time of measurement reducing the background normally associated with frequent high power operations.

It was desirable to approximate as closely as possible the conditions of a source in a cylindrical duct surrounded by an infinite attenuating medium. This of course required axial symmetry about the source. The geometry of the investigation lended itself naturally to cylindrical coordinates with the centerline of the duct as the axis.

The symmetry was investigated by making a number of counts at various positions about the axis and at constant vertical distances from the source. The source was placed 2½ ft from three of the tank walls and 3½ ft from the fourth (north) wall. The source was at a depth of 44 in.

The count rates near the close walls were 2-3 percent higher than those obtained for the same radius on the north radial. This increased count rate could be attributed to the proximity of the walls and change in orientation between the detector and source. Positions below the plane of the source registered count rates at low energy that were 10 percent higher than corresponding positions above the plane of source. This was attributed to the 4-in. diameter probe that

positioned the detector. When the detector was below the plane of the source the probe provided more scattering effect to the detector. The effect of the probe would not be so great above the source as below the source.

The effect of scattering by water and scattering by the detector body was compared outside the tank. The plexiglass case was filled with water placed between a detector and a Cesium-137 source and an energy spectrum measured. A detector body was placed in the dry case and the spectrum measured for various configurations of the detector. The configuration determined to be closest to that of the water was the complete detector less the lead ring about the lucite light pipe. This detector was placed in the water and count rates made with the detector facing in opposite directions. The count rates with the detector pointing away from a radiation source were about 1 percent higher than those pointing toward the source.

Departure from symmetrical conditions could be attributed to the detector, the positioning probe, the tank walls, and the lead ballast at the bottom of the duct. Neglecting these conditions and assuming an infinite medium introduced a small but acceptable error. A second source of error accepted was the assumption that the plexiglass case about the detector crystal attenuated the radiation the same as water. The density and electron density of plexiglass is very nearly the same as water.

Prior to making the measurements pertinent to the investigation the crystal was removed from the detector, the assembly checked for

leakage of light to the photomultiplier and the preamplifier checked for high voltage noise. No contribution to the count rate was determined. The crystal was replaced. The detector, analyzer and scaler were recalibrated with a Cesium-137 source. A complete Cesium photopeak was established and a resolution of 15% was determined for the gain and window width selected for the spectrum. Cesium was used for calibration because it represented the midpoint energy, 662 kev, of the Cobalt-60 spectrum.

The duct was placed in the tank and the source lowered into position. The exact vertical and horizontal position of the source was determined by making a vertical and horizontal survey with the analyzer set at the energy of the primary Cobalt-60 photon. The position of the source was considered the origin of the cylindrical coordinates. Changes in the detector position were made relative to the source.

An energy spectrum was measured at each selected position in the tank. A window width of 100 kev was used for the energy interval. Count rates were measured for each 100-kev interval up to 1.400 Mev. Counts were taken for 1 minute. A spectrum was measured for 7 points along each of 4 radial lines extending from the duct centerline. The radials selected were 15, 30, 50 and 75 cm above the source as in Figure 2. The points measured on each radial were 5, 7, 10, 15, 25, 35 and 55 cm from the duct centerline. Three points were measured along a radial in the plane of the source 20, 35 and 55 cm from the duct centerline.

In order to check the technique of this investigation, the experiment described by Collins (2) was duplicated as closely as possible.

The detector was placed pointed downward 3 in. above the water surface. The source was placed in the duct 12 in. below the water surface. Radial measurements were made 0, 6, 11, 16 and 21 cm from the duct centerline. The measurement on the centerline required positioning the crystal partly into the mouth of the duct. Two measurements near the duct boundary were approximated by making measurements above the duct mouth and normalizing to the measurements at the centerline.

A third variation of this experiment was conducted without the duct. The source was enclosed in a small plastic waterproof capsule and lowered into the tank. Measurements were made along a horizontal line 30 cm above the source. The results of this arrangement were compared with values theoretically determined.

ASSUMPTIONS AND CALCULATIONS

Background and coincidence corrections were applied to the count rates. Corrected count rates are tabulated in Tables 2 through 43 in the appendix. In order to transform the count rate into a dose rate it was necessary to, first, determine the rate that photons were striking the crystal and, secondly, transform the photon rate into a gamma flux and then to a dose rate.

The detector was assumed to be an isotropic detector, that is, the particles were measured equally, irrespective of their direction of travel. This assumption was an approximation in this case because of two conditions. The first condition involved the replacement of the volume of water with the volume of the detector body adjacent to the crystal. The second condition involved the detector crystal shape. The crystal did not present exactly the same cross sectional area nor the same thickness in all directions. Preliminary count rates measured in the water tank with various orientations between source and detector supported the validity of assuming an isotropic detector. An ideal isotropic detector presents an area that has a normal always pointed in the direction of motion of the photons being counted. This is a property of a sphere. An equivalent sphere for this cylindrical crystal was assumed to have a cross sectional area of 1.0 square in.

Conversion of count rate to number of photons striking the crystal per unit time required the use of two ratios calculated and tabulated by Miller and Snow (5). The interaction ratio is the ratio

of the number of gammas that interact at least once to the number that enter the crystal. The photofraction is the fraction of interacting gammas that is completely absorbed. The fraction of the gammas having a particular energy and are counted at that energy is the product of the photofraction and the interaction ratio. These ratios were calculated by a Monte Carlo method that simulated actual processes undergone by incident gamma rays and all subsequent radiation. The ratios vary with energy, position of source and size of crystal. The ratios were plotted versus energy for a 1 in. by 1 in. high crystal with the source on the face of the crystal. Appropriate values of the two ratios for the experimental energy intervals were estimated from this curve.

The product of the two ratios did not lead immediately to a conversion from count rate to photon rate over all of the energy spectrum. The highest primary energy of Cobalt-60 was first considered. The count rate at the differential energy interval that included the highest energy Cobalt-60 gamma represented those photons that were completely absorbed within the crystal. The number of photons per min having this amount of energy that struck the crystal was determined by the product of the count rate, the reciprocal of the photofraction and the reciprocal of the interaction ratio. The total number of photons per min that actually interacted with the crystal was the product of the count rate and the reciprocal of the photofraction. The difference between the number of photons interacting on the crystal and the number counted represented the photons that

lost only a portion of their energy while interacting with the crystal. These photons were visualized as entering the crystal, experiencing one or more scattering events and escaping from the crystal prior to complete absorption. These photons were actually counted at lower energies and consequently contributed to increasing the count rate at the lower energies. This phenomenon of contributing to lower energy count rates by higher energy photons was significant and required compensation. The contribution to measured count rates from photons of a particular energy interval was assumed to be equally distributed among the lower energy intervals. This assumption neglected the forward scattering effect characteristic of high energy photons and any influence of crystal size and shape on this phenomenon. The following develops a relation for the adjustment applied to the count rate of any energy interval:

i = energy interval subscript ($i = 1, 2, \ldots 14$)

r = interaction ratio

f = photofraction

N = corrected count rate, cpm

N' = adjusted count rate, cpm

Q = photon rate, photons per min

A = adjustment to the count rate, cpm

j = energy subscript ($j = 1, 2, \ldots i-1$)

$$A_j = \frac{(Nr)_j - N'_j}{1h - j} \qquad (A_0 = 0)$$

$$N'_i = N_i - \sum_{1}^{i-1} A_j$$

$$N_i = \frac{N'_i}{fr}$$

The development of the above relations was based on the equality of the corrected count rate and the adjusted rate for the highest energy interval (i = 1). The above equations were applied in turn to each energy interval commencing with the highest interval to determine the photon rate incident on the crystal. These calculations were made for the energy spectrum at each point under investigation. The photon rate incident on the crystal was tabulated in Tables 2 through 43.

The dose rate at a position was determined from equation 5-29 in Goldstein (3):

$$D(\vec{r}) = K \int_E u_a(E) I_0(\vec{r}, E) dE$$

K = constant dependent on the units desired

$u_a(E)$ = true (energy) absorption coefficient for air

$I_0(\vec{r}, E) = E N_0(\vec{r}, E)$ = energy flux per unit energy

$N_0(\vec{r}, E)dE$ = number flux of photons with energies between E and E + dE, photons per cm^2-sec

The following approximation was made:

$$D(\vec{r}) = K \sum_{1}^{14} u_a(E_i) E_i N_0(\vec{r}, E_i) \Delta E$$

The energy interval ΔE was 100 kev. The i-th energy was taken as the midpoint energy of each interval, that is, the base setting of the analyser plus one-half the window width. The number flux was determined from photon rate and the assumed 1.0 square in. cross section. The dose rate in mr/hr for each i-th energy interval is tabulated in Tables 2 through 43. The integrated dose rate at each experimental point is tabulated in Tables 1, 44 and 45.

The statistical error was treated as described in Price (8). Periodic tests were made to check the randomness of the measurements. The standard deviation was determined for the corrected count rate, the photon rate and dose rate. The maximum standard deviation for the integrated dose rate was 2.3 per cent at the furthest point from the source. The minimum standard error was 0.14 per cent at the closest point to the source.

RESULTS AND DISCUSSION

The dose rate versus radial distance from the duct centerline is plotted in Figure 3 for each radial. The position of the measurement was taken as the center of the crystal volume. Since the volume was finite the closest measurement to the duct occurred with the crystal face flush against the tube. The radial in the plane of the source was not investigated any closer to the duct than 20 cm because of the high count rates that were obtained. The increasing magnitude of the slope at this radial suggested the normal increase of dose rate as the radius from the source decreased. The influence of the duct was apparent in the successively higher radials. The duct influenced the dose rate close to the duct proportionately more and more as the vertical distance increased. This was due to the photons streaming through the duct. More photons of higher energy were able to travel up the duct and be scattered to the positions along the radials than would have been the case had they traveled entirely through the water medium.

Figure 4 is similar to Figure 3 except that the radial distance from the duct centerline is held constant while the dose rate is plotted versus vertical distance. The centerline of the duct, that is the radius equal to zero, was not measured. All the curves of Figure 4 should rise to a finite maximum at the plane of the source and fall off as vertical distance falls below the source. This maximum was demonstrated by the curves representing radial distances of

Figure 3. Dose rate as a function of radial distance from duct centerline

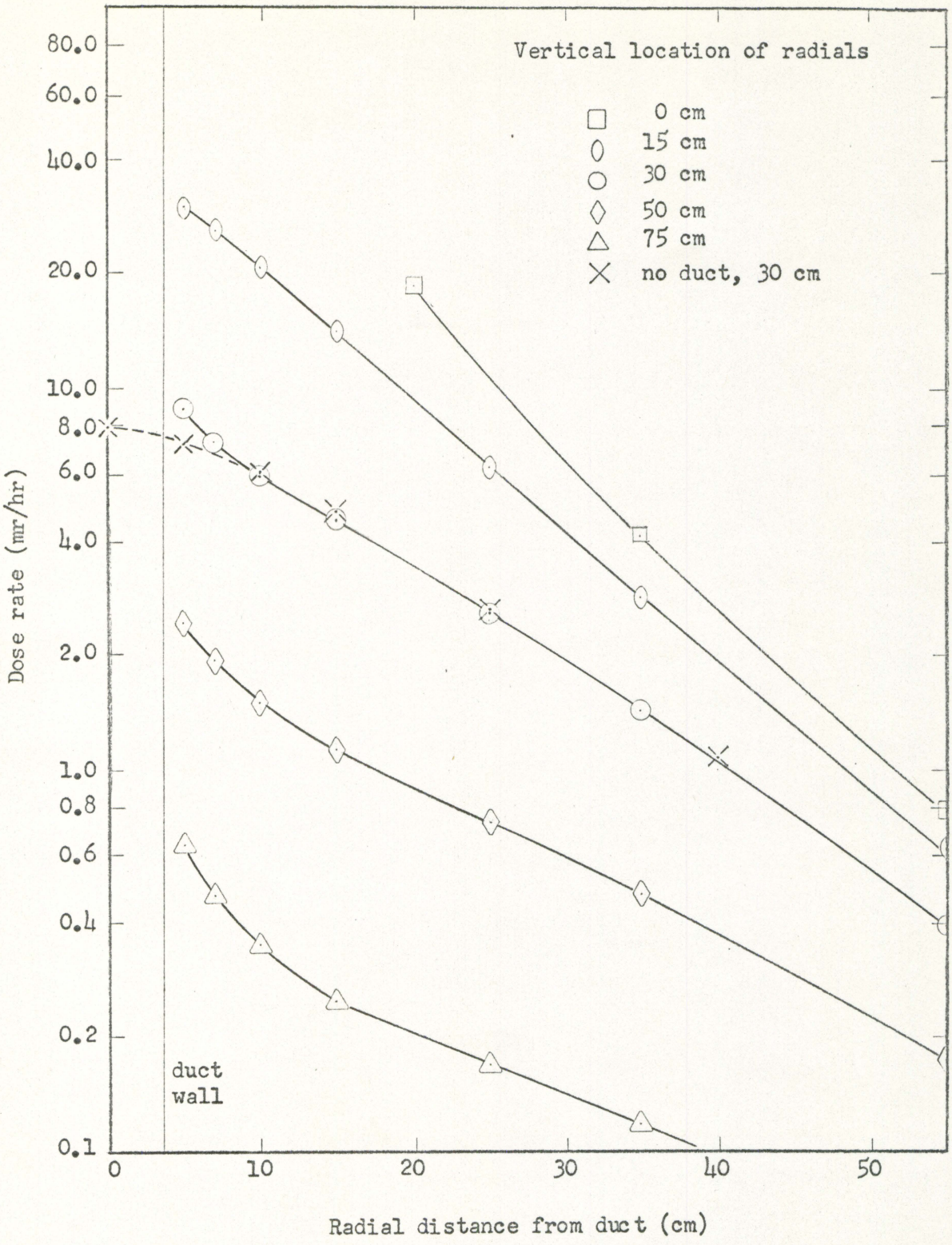
Vertical location of radials
0 cm
15 cm
30 cm
50 cm
75 cm
no duct, 30 cm
80.0
60.0
40.0
20.0
10.0
8.0
6.0
4.0
2.0
1.0
0.8
0.6
0.4
0.2
0.1
Dose rate (mr/hr)
duct
wall
0
10
20
30
40
50
Radial distance from duct (cm)

Figure 4. Dose rate as a function of vertical distance from the source

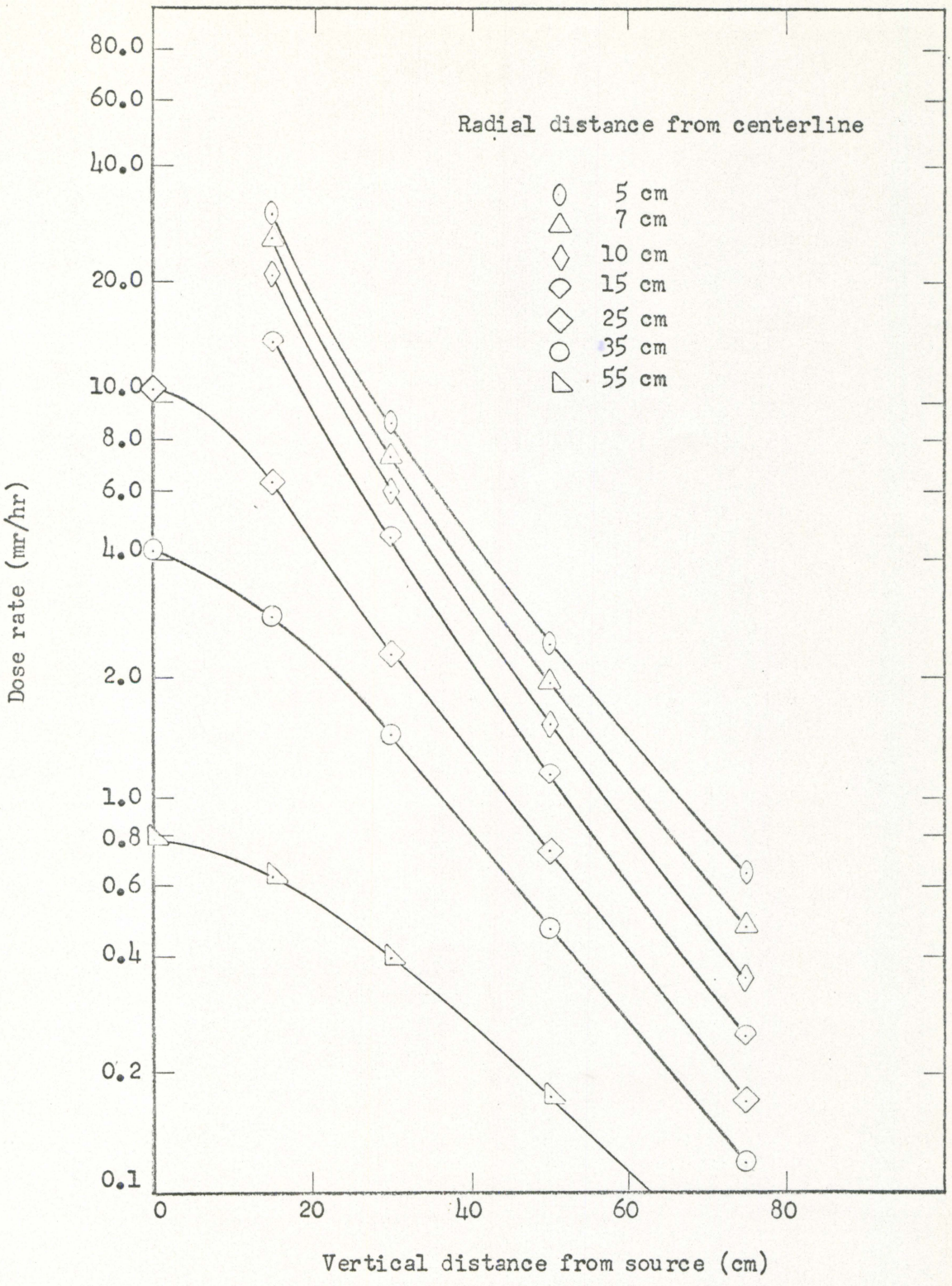
Radial distance from centerline
5 cm
7 cm
10 cm
15 cm
25 cm
35 cm
55 cm
80.0
60.0
40.0
20.0
10.0
8.0
6.0
4.0
2.0
1.0
0.8
0.6
0.4
0.2
0.1
Dose rate (mr/hr)
0
20
40
60
80
Vertical distance from source (cm)

25, 35 and 55 cm. Points closer than 20 cm along the radial in the plane of the source were not measured because of high count rates.

Figure 3 compared the radiation field with the duct and without the duct at a vertical distance of 30 cm. The disturbance in the field for this radial began at about 10 cm radial distance. This was equivalent to an angle of 19 degrees from the duct centerline with the source as the origin. Similar plane angles of 15, 30 and 45 degrees were investigated by cross plotting from Figure 3. Figure 5 shows the variation of dose rate with distance from the source for each of the three plane angles. In addition, the dose rate was plotted for a point source in an infinite medium using build up factors as contained in Murray (6). The 30 and 45 degree positions fell along the same curve. This indicated the effect of the void did not extend beyond the 30 degree angle. The 15 degree positions indicated that the void does effect the gamma field to at least this angle from the duct centerline. As expected, the curve representing 15 degrees and the curve representing 30 and 45 degrees began merging at distances close to the source. The curve, calculated from build up factors, was included to compare theoretical dose rates with measured dose rates at distances uneffected by the duct. Although differing somewhat in magnitude the calculated and the measured curve agree in shape and relation with distance.

Figure 6 compares values measured by experiment with values calculated from build up factors. The experimental dose rate referred to that measured without the duct and along a horizontal line originating

Figure 5. Dose rate as a function of radial distance from the source

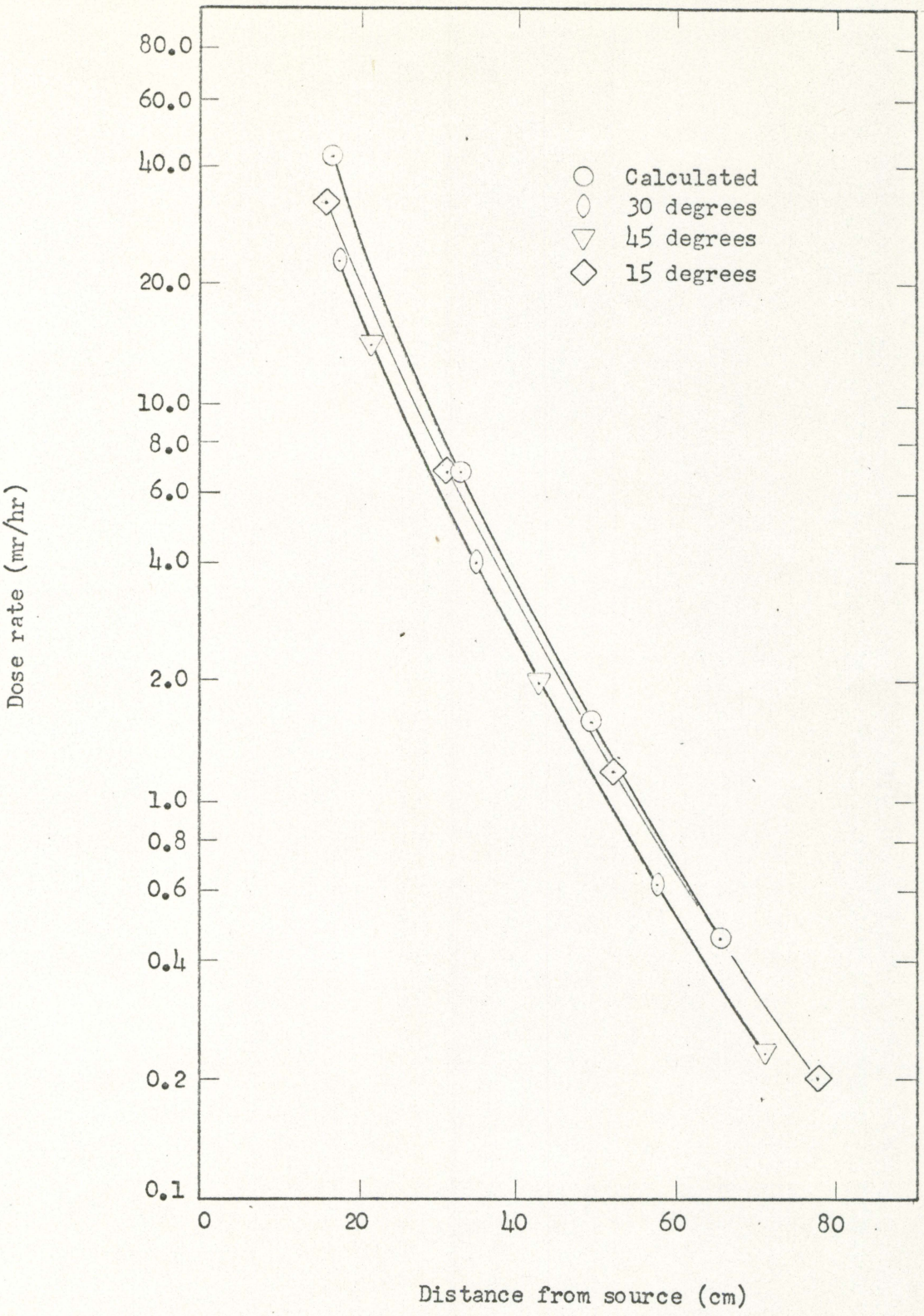
80.0
60.0
40.0
20.0
10.0
8.0
6.0
4.0
2.0
1.0
0.8
0.6
0.4
0.2
0.1
0
20
40
60
80
Calculated
30 degrees
45 degrees
15 degrees
Dose rate (mr/hr)
Distance from source (cm)

Figure 6. Experimental and calculated dose rates without the duct

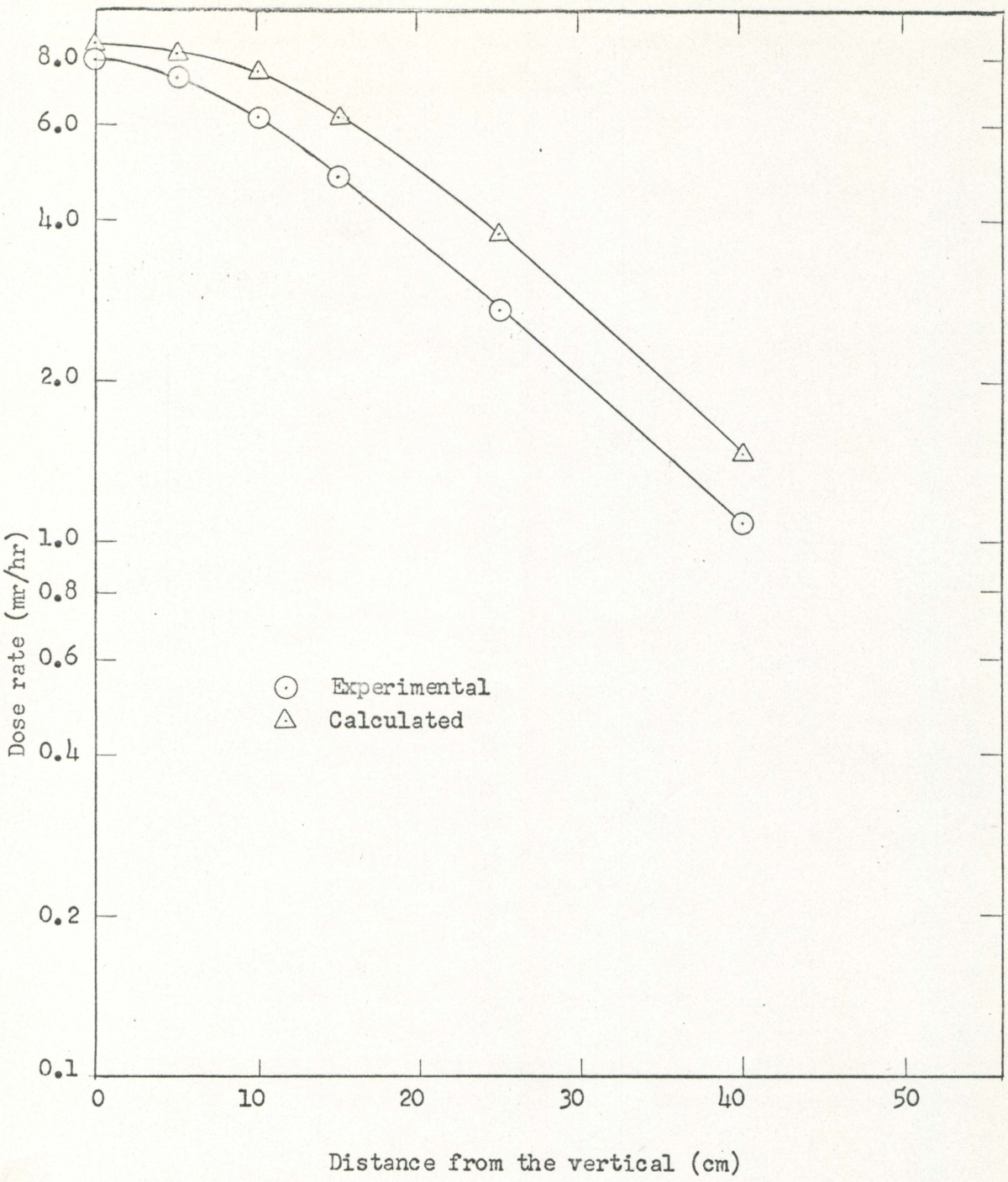
8.0
6.0
4.0
2.0
1.0
0.8
0.6
0.4
0.2
0.1
Dose rate (mr/hr)
Experimental
Calculated
0
10
20
30
40
50
Distance from the vertical (cm)

30 cm above the source. This line duplicated the 30 cm radial in the duct measurement. The calculated dose rate referred to that calculated from buildup factors assuming an isotropic point Cobalt-60 source in an infinite water medium. The difference between calculated data and measured data varies from 6.5 percent directly above the source to 25.7 percent at the furthest point measured. This is a reasonable variation between measured and calculated dose rates. Loevinger, Japha and Brownell (4) estimated the accuracy of dose buildup factors to range from 5 to 30 percent. These buildup factors were calculated by Goldstein and tabulated in (3), (4) and (6).

The final portion of the investigation involved the attempt to duplicate the results of Collins (2). The primary difference between the geometry of Collins' experiment and that of this experiment was the extension of the duct out of the water. The construction of the tube used for this duct required that it extend out of the water a minimum of 2 3/4 in. The duct used by Collins was approximately flush with the surface of the water. In addition, the source used by Collins was 444-mc and was positioned at the center line of the duct on one side of a water shield with the detector positioned on the other side. The source of this investigation was surrounded by water, except for the duct, above and below the source. The type of detector used by Collins was unknown. Results from Collins (2) were normalized to the strength of the source used in this experiment. The comparison, indicated by Figure 7, was in close agreement near the duct. At 30 cm from the duct

Figure 7. Comparison of experimental measurements

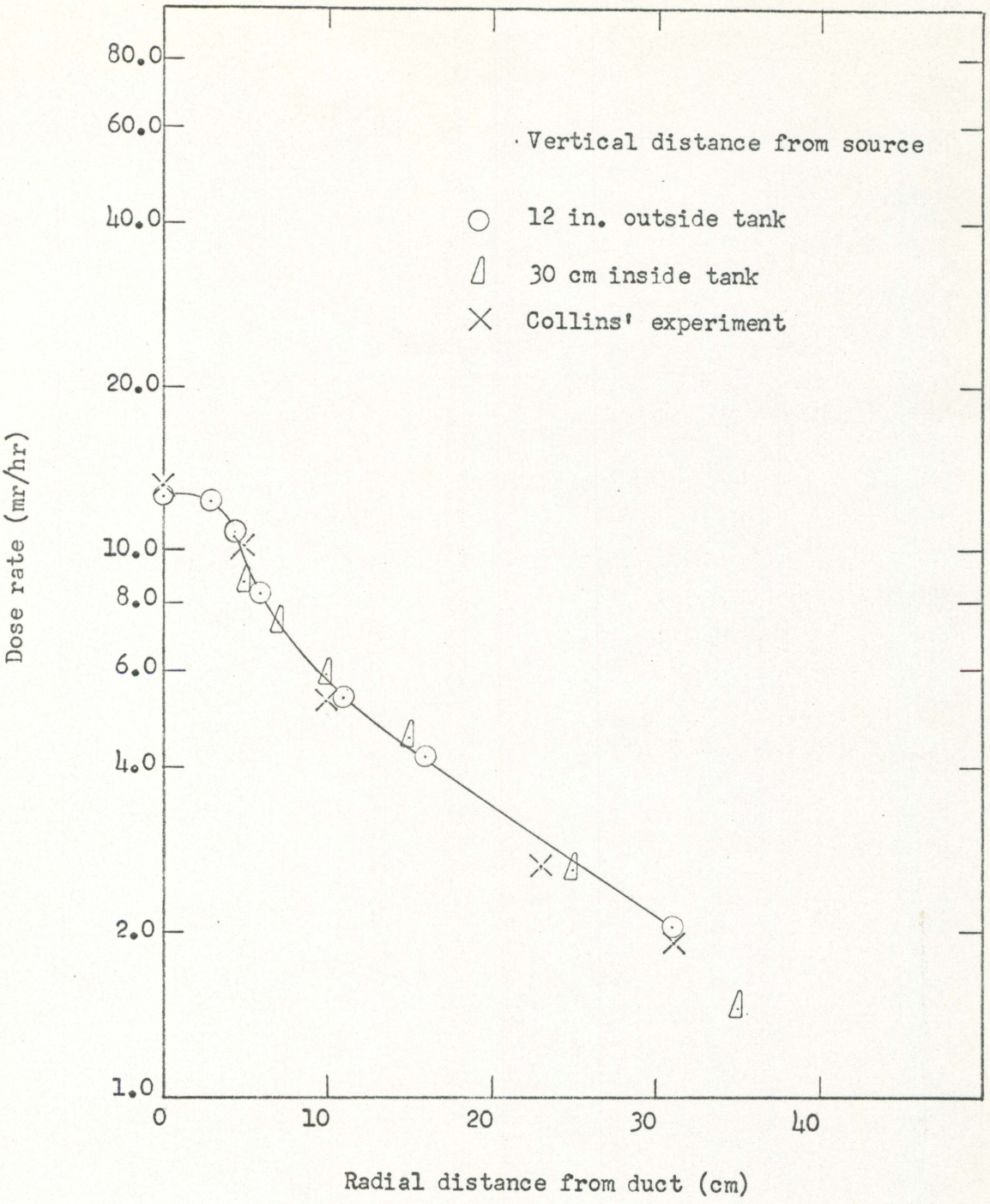
80.0
60.0
40.0
20.0
10.0
8.0
6.0
4.0
2.0
1.0
0
10
20
30
40
Dose rate (mr/hr)
Radial distance from duct (cm)
Vertical distance from source
12 in. outside tank
30 cm inside tank
Collins' experiment

centerline agreement was within 10 percent. The higher dose rate for this experiment at 30 cm probably resulted from the scattering medium below the source. This effect was not as noticeable near the duct since the dose rate was more dependent on uncollided photons or photons near the uncollided energy. Figure 7 also compares the experimental dose rate taken out of the water with the dose rate from the corresponding 30 cm radial measured in the water medium. The close agreement indicated that the measurement taken outside the shielding medium could be used in lieu of the measurement made within the medium.

The agreement with theory in one case and an independent experiment in a second case justifies confidence in the measured dose rates. These rates are suitable for comparison with analytical techniques developed to predict the effect of a duct.

AREAS FOR FURTHER RESEARCH

A number of areas for future investigation became apparent as this experiment progressed. In Figure 3 the effect of the duct became more pronounced as distance along the duct increased. This effect should be investigated using ducts of other diameters. Results from such an investigation would demonstrate any effect due to the duct size.

Figure 7 indicated, for one radial, that dose rates measured outside the shielding medium were in close agreement with those measured in the medium. Before this agreement could be generally accepted for all radials, an investigation should be made with various thicknesses of the medium. The use of different attenuating mediums would further broaden the investigation. Verification of agreement between measurements inside and outside the medium would reduce the need for making measurements within a medium during investigation of ducts. A further area of study would be the effect of source energy on the gamma field about a duct. This same investigation could be conducted using other sources. Gamma radiation from the reactor thermal column could be investigated with various types of ducts including ducts with bends, elbows and obstructions, and multiple ducts.

CONCLUSIONS

From this experiment the following conclusions may be stated:

1. The presence of a duct in a shielding medium increased the dose rate in the vicinity of the duct.

2. Dose rates for the gamma field influenced by a duct approached the values for no duct as the distance from the duct increased. Dose rates reached the limiting (no duct) dose rate within 30 degrees of the duct centerline.

3. The influence of the duct was more pronounced as the distance along the duct increased.

4. This tank facility was a suitable infinite water medium. The experimental geometry was satisfactorily symmetrical.

5. This detector and counting equipment satisfactorily determined differential dose rates as low as 0.005 mr/hr and integrated dose rates as low as 0.1 mr/hr.

6. The application of the photofraction and interaction ratio was successful in converting count rate to dose rate.

7. Measurements made outside the shielding medium may approximate those made inside the medium for the same shield thickness, and should be investigated more thoroughly for confirmation.

8. The integrated dose rates were sufficiently accurate to provide experimental comparison for theoretically determined rates.

LITERATURE CITED

1. Clark, M.D., Etherington, H.W., Greenaway, D.S., and Paterson, W.J. Streaming of scattered gamma radiation through a duct in a shield. American Nuclear Society Trans. 5: 395. 1962.

2. Collins, D.G. An application of Monte Carlo methods to duct-streaming research. American Nuclear Society Trans. 5: 396. 1962.

3. Goldstein, Herbert. Fundamental aspects of reactor shielding. Reading, Mass., Addison-Wesley Publishing Co., Inc. 1959.

4. Loevinger, R., Japha, E.M., and Brownell, G.L. Discrete radioisotope sources. In Hine, Gerald J. and Brownell, Gordon L., eds. Radiation dosimetry. pp 693-799. New York, N.Y., Academic Press Inc. 1956.

5. Miller, W.F. and Snow, William J. NaI and CsI efficiencies and photofractions for gamma-ray detection. Nucleonics 19, No. 11: 174-175. Nov. 1961.

6. Murray, Raymond L. Introduction to nuclear engineering. 2nd ed. Englewood Cliffs, N.J., Prentice-Hall, Inc. 1961.

7. Pratt, William W. and Kouts, Herbert J. Leakage of gamma radiation through spherical and cylindrical voids. U.S. Atomic Energy Commission Report BNL-1328 (Brookhaven National Laboratory, Upton, New York). 1952.

8. Price, William J. Nuclear radiation detection. New York, N.Y., McGraw-Hill Book Co., Inc. 1958.

ACKNOWLEDGMENTS

Completion of this investigation would have been impossible without the direction and assistance of Dr. Glenn Murphy and Mr. D.S. Seaacer. The opportunity for advanced study was provided by the U.S. Naval Postgraduate Educational Program.

I wish to express my gratitude for the encouragement and patient endurance of my family throughout this investigation and the past three years of study.

APPENDIX

Table 1. Integrated dose rate

Vertical distance from source (cm)	Radial distance from duct (cm)	Dose rate (mr/hr)	Standard deviation (mr/hr)
0	20	18.386	0.031
0	35	4.172	0.013
0	55	0.777	0.005
15	5	30.612	0.042
15	7	26.466	0.041
15	10	20.689	0.034
15	15	14.111	0.027
15	25	6.238	0.017
15	35	2.870	0.010
15	55	0.630	0.005
30	5	8.785	0.022
30	7	7.277	0.019
30	10	5.902	0.016
30	15	4.516	0.013
30	25	2.583	0.009
30	35	1.433	0.007
30	55	0.392	0.003
50	5	2.430	0.009
50	7	1.918	0.008
50	10	1.509	0.007
50	15	1.130	0.006
50	25	0.732	0.005
50	35	0.469	0.004
50	55	0.171	0.002
75	5	0.6385	0.0051
75	7	0.4635	0.0036
75	10	0.3510	0.0031
75	15	0.2483	0.0026
75	25	0.1668	0.0020
75	35	0.1187	0.0017
75	55	0.0604	0.0014

Table 2. Experimental energy spectrum

Position: vertical 75 cm
radial 5 cm

Gamma energy (Mev)	Corrected count rate (cpm)	Standard deviation (cpm)	Photon rate (photons per min)	Standard deviation (photons per min)	Dose rate (mr/hr)	Standard deviation (mr/hr)
1.350	422	14	9,336	310	0.0592	0.0020
1.250	680	26	11,290	432	0.0679	0.0026
1.150	1,157	34	16,528	486	0.0915	0.0027
1.050	1,304	36	11,676	322	0.0607	0.0017
0.950	1,726	41	12,608	299	0.0593	0.0014
0.850	2,397	49	14,905	305	0.0645	0.0013
0.750	2,548	50	8,548	168	0.0326	0.0006
0.650	3,128	56	8,785	157	0.0298	0.0005
0.550	3,953	63	9,500	152	0.0273	0.0004
0.450	4,924	70	9,058	129	0.0213	0.0003
0.350	7,975	89	13,706	153	0.0214	0.0003
0.250	16,607	129	22,415	174	0.0270	0.0002
0.150	41,458	204	40,862	201	0.0253	0.0001
0.050	87,159	295	77,165	261	0.0477	0.0002

Table 3. Experimental energy spectrum

Position: vertical 75 cm
radial 7 cm

Gamma energy (Mev)	Corrected count rate (cpm)	Standard deviation (cpm)	Photon rate (photons per min)	Standard deviation (photons per min)	Dose rate (mr/hr)	Standard deviation (mr/hr)
1.350	285	12	6,305	266	0.0398	0.0017
1.250	404	20	6,409	158	0.0386	0.0009
1.150	683	26	9,543	363	0.0528	0.0020
1.050	797	28	7,303	256	0.0380	0.0013
0.950	1,092	33	8,405	254	0.0395	0.0012
0.850	1,508	39	9,511	246	0.0411	0.0011
0.750	1,876	43	8,397	193	0.0321	0.0007
0.650	2,254	47	7,041	147	0.0239	0.0005
0.550	2,897	54	7,500	140	0.0216	0.0004
0.450	4,024	63	8,767	137	0.0206	0.0003
0.350	6,697	82	12,430	152	0.0222	0.0003
0.250	14,261	119	19,820	165	0.0238	0.0002
0.150	37,782	194	37,953	195	0.0235	0.0001
0.050	82,351	288	74,293	258	0.0460	0.0001

Table 4. Experimental energy spectrum

Position: vertical 75 cm
radial 10 cm

Gamma energy (Mev)	Corrected count rate (cpm)	Standard deviation (cpm)	Photon rate (photons per min)	Standard deviation (photons per min)	Dose rate (mr/hr)	Standard deviation (mr/hr)
1.350	276	11	4,956	235	0.0313	0.0015
1.250	259	11	3,785	161	0.0228	0.0010
1.150	447	21	6,112	287	0.0339	0.0016
1.050	519	23	4,663	207	0.0243	0.0011
0.950	747	27	6,030	218	0.0284	0.0010
0.850	1,008	32	6,467	205	0.0279	0.0009
0.750	1,285	36	6,002	168	0.0230	0.0006
0.650	1,728	42	6,463	157	0.0220	0.0005
0.550	2,224	47	6,300	133	0.0181	0.0004
0.450	3,112	56	7,103	128	0.0168	0.0003
0.350	5,365	73	10,324	141	0.0184	0.0002
0.250	11,930	109	17,002	155	0.0205	0.0002
0.150	32,759	181	33,310	184	0.0205	0.0001
0.050	76,586	276	69,476	250	0.0431	0.0001

Table 5. Experimental energy spectrum

Position: vertical 75 cm
radial 15 cm

Gamma energy (Mev)	Corrected count rate (cpm)	Standard deviation (cpm)	Photon rate (photons per min)	Standard deviation (photons per min)	Dose rate (mr/hr)	Standard deviation (mr/hr)
1.350	90	4	1,991	88	0.0126	0.0005
1.250	155	12	2,624	203	0.0158	0.0012
1.150	291	17	4,366	255	0.0247	0.0014
1.050	354	19	3,545	190	0.0184	0.0010
0.950	470	22	3,621	169	0.0171	0.0008
0.850	657	25	4,198	160	0.0181	0.0007
0.750	814	28	3,651	125	0.0140	0.0005
0.650	1,114	33	4,187	124	0.0142	0.0004
0.550	1,567	40	4,900	125	0.0141	0.0004
0.450	2,398	49	6,152	126	0.0145	0.0003
0.350	4,152	64	8,345	129	0.0149	0.0002
0.250	9,414	97	13,661	141	0.0165	0.0002
0.150	26,488	163	27,154	167	0.0169	0.0001
0.050	65,450	256	59,875	234	0.0371	0.0001

Table 6. Experimental energy spectrum

Position: vertical 75 cm
radial 25 cm

Gamma energy (Mev)	Corrected count rate (cpm)	Standard deviation (cpm)	Photon rate (photons per min)	Standard deviation (photons per min)	Dose rate (mr/hr)	Standard deviation (mr/hr)
1.350	53	4	1,173	88	0.0074	0.0005
1.250	97	7	1,656	155	0.0100	0.0009
1.150	139	12	1,850	160	0.0103	0.0009
1.050	207	14	2,312	156	0.0120	0.0008
0.950	304	17	2,724	152	0.0128	0.0007
0.850	442	21	3,125	148	0.0135	0.0006
0.750	587	24	3,023	123	0.0116	0.0005
0.650	773	28	2,950	107	0.0100	0.0004
0.550	1,018	32	2,994	94	0.0086	0.0003
0.450	1,637	40	4,260	104	0.0100	0.0002
0.350	2,829	53	5,709	107	0.0102	0.0002
0.250	6,229	79	8,974	114	0.0108	0.0001
0.150	18,780	139	19,404	143	0.0120	0.0001
0.050	48,486	220	44,646	202	0.0276	0.0001

Table 7. Experimental energy spectrum

Position: vertical 75 cm
radial 35 cm

Gamma energy (Mev)	Corrected count rate (cpm)	Standard deviation (cpm)	Photon rate (photons per min)	Standard deviation (photons per min)	Dose rate (mr/hr)	Standard deviation (mr/hr)
1.350	32	4	708	88	0.0045	0.0005
1.250	59	8	1,011	137	0.0061	0.0008
1.150	122	11	1,892	170	0.0105	0.0009
1.050	148	12	1,503	121	0.0078	0.0006
0.950	193	14	1,462	106	0.0069	0.0005
0.850	275	17	1,780	110	0.0077	0.0005
0.750	409	20	2,275	111	0.0087	0.0004
0.650	603	25	2,669	111	0.0091	0.0004
0.550	762	28	2,313	85	0.0067	0.0002
0.450	1,168	34	2,964	86	0.0070	0.0002
0.350	2,117	46	4,218	92	0.0074	0.0002
0.250	4,669	58	6,706	83	0.0081	0.0001
0.150	12,882	114	13,135	116	0.0081	0.0001
0.050	35,341	188	32,454	173	0.0201	0.0001

Table 8. Experimental energy spectrum

Position: vertical 75 cm
radial 55 cm

Gamma energy (Mev)	Corrected count rate (cpm)	Standard deviation (cpm)	Photon rate (photons per min)	Standard deviation (photons per min)	Dose rate (mr/hr)	Standard deviation (mr/hr)
1.350	18	3	398	66	0.0025	0.0004
1.250	44	7	796	127	0.0048	0.0008
1.150	67	8	956	114	0.0053	0.0006
1.050	107	10	1,291	121	0.0067	0.0006
0.950	100	10	498	50	0.0023	0.0002
0.850	132	11	646	55	0.0029	0.0002
0.750	211	15	1,159	82	0.0044	0.0003
0.650	244	16	818	54	0.0028	0.0002
0.550	362	19	1,114	60	0.0033	0.0002
0.450	643	25	1,825	71	0.0043	0.0002
0.350	1,110	33	2,315	69	0.0041	0.0001
0.250	2,269	48	3,233	68	0.0039	0.0001
0.150	5,824	76	5,860	76	0.0036	0.0001
0.050	16,650	129	15,338	119	0.0095	0.0001

Table 9. Experimental energy spectrum

Position: vertical 50 cm
radial 5 cm

Gamma energy (Mev)	Corrected count rate (cpm)	Standard deviation (cpm)	Photon rate (photons per min)	Standard deviation (photons per min)	Dose rate (mr/hr)	Standard deviation (mr/hr)
1.350	2,052	32	45,398	708	0.287	0.004
1.250	2,675	36	41,161	563	0.247	0.003
1.150	4,755	69	67,318	977	0.373	0.005
1.050	4,663	68	34,220	498	0.178	0.003
0.950	6,381	80	44,967	564	0.212	0.003
0.850	8,687	93	51,970	556	0.225	0.002
0.750	9,520	98	33,120	341	0.127	0.001
0.650	11,063	105	28,215	267	0.096	0.001
0.550	14,014	118	32,406	272	0.093	0.001
0.450	19,161	138	39,126	282	0.092	0.001
0.350	30,230	174	52,909	304	0.094	0.001
0.250	64,368	254	87,994	347	0.106	0.001
0.150	165,508	407	164,605	405	0.102	0.001
0.050	357,760	599	318,997	534	0.198	0.001

Table 10. Experimental energy spectrum

Position: vertical 50 cm
radial 7 cm

Gamma energy (Mev)	Corrected count rate (cpm)	Standard deviation (cpm)	Photon rate (photons per min)	Standard deviation (photons per min)	Dose rate (mr/hr)	Standard deviation (mr/hr)
1.350	1,339	26	29,624	576	0.187	0.004
1.250	1,839	30	28,882	478	0.174	0.003
1.150	3,219	57	45,572	807	0.252	0.004
1.050	3,476	59	29,306	497	0.153	0.003
0.950	4,734	69	34,967	510	0.165	0.002
0.850	6,286	79	37,133	466	0.161	0.002
0.750	7,341	86	28,646	335	0.109	0.001
0.650	8,559	93	23,438	255	0.090	0.001
0.550	11,359	107	29,100	274	0.084	0.001
0.450	16,000	127	35,220	279	0.083	0.001
0.350	26,443	162	48,988	311	0.087	0.001
0.250	57,376	240	80,265	336	0.097	0.001
0.150	152,873	391	153,937	395	0.096	0.001
0.050	341,868	585	307,526	526	0.190	0.001

Table 11. Experimental energy spectrum

Position: vertical 50 cm
radial 10 cm

Gamma energy (Mev)	Corrected count rate (cpm)	Standard deviation (cpm)	Photon rate (photons per min)	Standard deviation (photons per min)	Dose rate (mr/hr)	Standard deviation (mr/hr)
1.350	881	30	19,491	464	0.123	0.003
1.250	1,309	36	21,118	580	0.127	0.003
1.150	2,259	47	32,100	668	0.177	0.004
1.050	2,568	51	23,121	458	0.120	0.002
0.950	3,362	58	24,286	419	0.114	0.002
0.850	4,578	68	27,663	411	0.120	0.002
0.750	5,492	74	22,730	306	0.087	0.001
0.650	6,825	83	21,628	263	0.074	0.001
0.550	8,908	94	23,719	250	0.068	0.001
0.450	13,335	116	31,552	274	0.074	0.001
0.350	22,143	149	42,258	284	0.075	0.001
0.250	49,467	222	70,424	316	0.085	0.001
0.150	135,942	369	138,206	376	0.086	0.001
0.050	318,235	564	288,711	511	0.179	0.001

Table 12. Experimental energy spectrum

Position: vertical 50 cm
radial 15 cm

Gamma energy (Mev)	Corrected count rate (cpm)	Standard deviation (cpm)	Photon rate (photons per min)	Standard deviation (photons per min)	Dose rate (mr/hr)	Standard deviation (mr/hr)
1.350	408	14	9,026	309	0.057	0.002
1.250	867	29	15,398	515	0.093	0.003
1.150	1,468	38	21,497	557	0.119	0.003
1.050	1,784	42	17,572	413	0.092	0.002
0.950	2,285	48	16,760	352	0.079	0.002
0.850	3,201	57	20,135	358	0.087	0.002
0.750	3,910	63	17,020	274	0.065	0.001
0.650	5,066	71	17,496	244	0.060	0.001
0.550	6,853	83	19,819	240	0.057	0.001
0.450	10,716	101	24,897	246	0.059	0.001
0.350	17,245	131	33,561	255	0.060	0.001
0.250	39,946	200	57,783	289	0.070	0.001
0.150	113,090	336	115,961	345	0.071	0.001
0.050	283,220	533	259,241	482	0.161	0.001

Table 13. Experimental energy spectrum

Position: vertical 50 cm
radial 25 cm

Gamma energy (Mev)	Corrected count rate (cpm)	Standard deviation (cpm)	Photon rate (photons per min)	Standard deviation (photons per min)	Dose rate (mr/hr)	Standard deviation (mr/hr)
1.350	218	10	4,823	221	0.0305	0.0014
1.250	510	23	9,226	416	0.0557	0.0025
1.150	794	28	11,476	404	0.0637	0.0022
1.050	1,064	33	11,329	351	0.0590	0.0018
0.950	1,377	37	10,631	255	0.0502	0.0012
0.850	1,931	44	12,405	283	0.0536	0.0012
0.750	2,424	49	11,094	224	0.0424	0.0009
0.650	3,217	57	11,736	208	0.0400	0.0007
0.550	4,471	67	13,644	204	0.0393	0.0006
0.450	6,766	82	17,045	206	0.0400	0.0005
0.350	11,843	109	23,779	219	0.0424	0.0004
0.250	26,765	164	38,789	238	0.0467	0.0003
0.150	78,541	280	80,972	289	0.0501	0.0002
0.050	206,899	455	190,706	419	0.1193	0.0003

Table 14. Experimental energy spectrum

Position: vertical 90 cm
radial 35 cm

Gamma energy (Mev)	Corrected count rate (cpm)	Standard deviation (cpm)	Photon rate (photons per min)	Standard deviation (photons per min)	Dose rate (mr/hr)	Standard deviation (mr/hr)
1.350	140	12	3,097	265	0.0196	0.0017
1.250	295	17	5,226	301	0.0314	0.0018
1.150	471	22	6,715	314	0.0372	0.0017
1.050	654	26	6,994	279	0.0365	0.0014
0.950	911	30	7,685	252	0.0359	0.0011
0.850	1,236	35	7,921	224	0.0343	0.0010
0.750	1,467	38	6,176	160	0.0238	0.0006
0.650	2,000	45	7,289	164	0.0248	0.0005
0.550	2,865	54	9,013	170	0.0260	0.0005
0.450	4,344	66	11,094	168	0.0261	0.0004
0.350	7,914	89	16,282	183	0.0290	0.0003
0.250	17,741	133	25,837	194	0.0310	0.0002
0.150	52,036	228	53,710	235	0.0329	0.0001
0.050	141,053	376	130,374	348	0.0808	0.0002

Table 15. Experimental energy spectrum

Position: vertical 50 cm
radial 55 cm

Gamma energy (Mev)	Corrected count rate (cpm)	Standard deviation (cpm)	Photon rate (photons per min)	Standard deviation (photons per min)	Dose rate (mr/hr)	Standard deviation (mr/hr)
1.350	38	6	841	133	0.0054	0.0009
1.250	116	11	2,194	208	0.0132	0.0012
1.150	141	12	1,809	154	0.0100	0.0008
1.050	214	15	2,370	166	0.0123	0.0009
0.950	291	17	2,425	142	0.0114	0.0007
0.850	389	20	2,446	126	0.0106	0.0005
0.750	586	24	3,272	134	0.0125	0.0005
0.650	710	27	2,554	97	0.0087	0.0003
0.550	1,091	33	3,644	110	0.0105	0.0003
0.450	1,662	41	4,363	107	0.0103	0.0002
0.350	2,865	53	5,794	107	0.0103	0.0002
0.250	6,498	80	9,446	116	0.0114	0.0001
0.150	19,633	140	20,340	145	0.0126	0.0001
0.050	55,661	236	51,685	219	0.0321	0.0001

Table 16. Experimental energy spectrum

Position: vertical 30 cm
radial 5 cm

Gamma energy (Mev)	Corrected count rate (cpm)	Standard deviation (cpm)	Photon rate (photons per min)	Standard deviation (photons per min)	Dose rate (mr/hr)	Standard deviation (mr/hr)
1.350	6,816	83	150,796	1,835	0.952	0.012
1.250	11,749	108	198,344	1,822	1.193	0.011
1.150	19,069	138	268,150	1,943	1.485	0.011
1.050	19,266	139	147,148	1,063	0.766	0.006
0.950	23,337	153	138,239	906	0.650	0.004
0.850	31,236	177	170,761	967	0.739	0.004
0.750	34,173	185	110,997	601	0.424	0.002
0.650	38,719	197	89,388	455	0.378	0.002
0.550	46,996	217	95,963	446	0.276	0.001
0.450	64,917	255	127,870	502	0.300	0.001
0.350	102,314	320	176,291	551	0.314	0.001
0.250	213,420	462	288,456	624	0.347	0.001
0.150	532,465	730	524,971	747	0.325	0.001
0.050	1,153,803	1,073	1,025,565	954	0.636	0.001

Table 17. Experimental energy spectrum

Position: vertical 30 cm
radial 7 cm

Gamma energy (Mev)	Corrected count rate (cpm)	Standard deviation (cpm)	Photon rate (photons per min)	Standard deviation (photons per min)	Dose rate (mr/hr)	Standard deviation (mr/hr)
1.350	5,016	71	110,973	1,570	0.701	0.010
1.250	9,286	96	159,720	1,650	0.960	0.010
1.150	14,474	120	201,247	1,667	1.111	0.009
1.050	15,360	124	124,663	1,005	0.648	0.005
0.950	13,603	117	113,704	837	0.535	0.004
0.850	25,065	158	139,986	883	0.606	0.004
0.750	28,062	168	97,378	583	0.372	0.002
0.650	32,136	179	79,124	441	0.269	0.001
0.550	40,496	201	91,400	453	0.253	0.001
0.450	56,449	238	116,789	492	0.275	0.001
0.350	92,301	304	166,152	547	0.296	0.001
0.250	196,213	443	270,376	609	0.325	0.001
0.150	500,114	708	497,744	705	0.308	0.001
0.050	1,114,748	1,056	997,897	945	0.618	0.001

Table 18. Experimental energy spectrum

Position: vertical 30 cm
radial 10 cm

Gamma energy (Mev)	Corrected count rate (cpm)	Standard deviation (cpm)	Photon rate (photons per min)	Standard deviation (photons per min)	Dose rate (mr/hr)	Standard deviation (mr/hr)
1.350	3,698	61	81,814	1,349	0.517	0.008
1.250	6,945	83	120,215	1,437	0.722	0.009
1.150	10,745	104	149,293	1,435	0.788	0.008
1.050	11,759	109	99,345	921	0.517	0.005
0.950	14,665	121	95,947	793	0.452	0.004
0.850	19,777	141	113,492	809	0.492	0.003
0.750	22,161	149	78,451	527	0.299	0.002
0.650	26,008	161	68,413	424	0.232	0.001
0.550	33,324	183	79,575	433	0.229	0.001
0.450	46,972	217	100,596	462	0.236	0.001
0.350	79,703	282	148,721	526	0.264	0.001
0.250	171,408	414	239,594	578	0.289	0.001
0.150	451,674	672	453,898	675	0.781	0.001
0.050	1,045,885	1,023	943,713	924	0.584	0.001

Table 19. Experimental energy spectrum

Position: vertical 30 cm
radial 15 cm

Gamma energy (Mev)	Corrected count rate (cpm)	Standard deviation (cpm)	Photon rate (photons per min)	Standard deviation (photons per min)	Dose rate (mr/hr)	Standard deviation (mr/hr)
1.350	2,430	35	54,867	774	0.347	0.005
1.250	4,702	69	81,355	1,193	0.489	0.007
1.150	7,625	87	108,337	1,236	0.600	0.007
1.050	8,485	92	74,489	807	0.388	0.004
0.950	10,499	102	69,203	672	0.396	0.003
0.850	14,446	120	85,394	709	0.370	0.003
0.750	16,496	128	61,809	479	0.236	0.002
0.650	19,573	140	54,281	388	0.184	0.001
0.550	25,365	159	63,056	395	0.181	0.001
0.450	37,085	193	83,771	435	0.192	0.001
0.350	63,389	252	120,961	480	0.215	0.001
0.250	138,612	372	196,048	526	0.236	0.001
0.150	377,667	615	332,780	625	0.237	0.001
0.050	913,789	956	830,863	869	0.515	0.001

Table 20. Experimental energy spectrum

Position: vertical 30 cm
radial 25 cm

Gamma energy (Mev)	Corrected count rate (cpm)	Standard deviation (cpm)	Photon rate (photons per min)	Standard deviation (photons per min)	Dose rate (mr/hr)	Standard deviation (mr/hr)
1.350	1,198	24	26,504	531	0.167	0.003
1.250	2,250	47	39,839	811	0.234	0.005
1.150	3,794	62	54,802	897	0.304	0.005
1.050	4,340	66	39,827	606	0.207	0.003
0.950	5,686	75	41,478	547	0.195	0.003
0.850	7,675	88	46,060	529	0.199	0.002
0.750	9,141	96	37,237	391	0.124	0.001
0.650	11,264	106	34,926	329	0.119	0.001
0.550	15,147	123	41,550	337	0.120	0.001
0.450	22,298	150	52,637	354	0.124	0.001
0.350	33,405	196	74,730	381	0.133	0.001
0.250	86,276	294	123,709	422	0.149	0.001
0.150	243,609	494	249,125	505	0.154	0.001
0.050	624,317	791	572,534	725	0.354	0.001

Table 21. Experimental energy spectrum

Position: vertical 30 cm
radial 35 cm

Gamma energy (Mev)	Corrected count rate (cpm)	Standard deviation (cpm)	Photon rate (photons per min)	Standard deviation (photons per min)	Dose rate (mr/hr)	Standard deviation (mr/hr)
1.350	588	17	13,009	376	0.082	0.002
1.250	1,123	34	19,462	588	0.117	0.004
1.150	1,784	42	25,114	591	0.139	0.003
1.050	2,176	47	20,983	453	0.109	0.002
0.950	2,890	54	21,927	409	0.103	0.002
0.850	3,896	62	23,736	378	0.103	0.002
0.750	4,936	70	22,275	316	0.085	0.001
0.650	6,282	79	21,521	271	0.073	0.001
0.550	8,489	92	24,444	265	0.070	0.001
0.450	12,441	112	29,825	268	0.070	0.001
0.350	22,309	149	44,585	298	0.080	0.001
0.250	50,172	224	72,515	324	0.087	0.001
0.150	146,340	382	150,643	393	0.093	0.001
0.050	388,539	623	358,195	576	0.222	0.001

Table 22. Experimental energy spectrum

Position: vertical 30 cm
radial 55 cm

Gamma energy (Mev)	Corrected count rate (cpm)	Standard deviation (cpm)	Photon rate (photons per min)	Standard deviation (photons per min)	Dose rate (mr/hr)	Standard deviation (mr/hr)
1.350	103	7	2,279	155	0.0144	0.0010
1.250	225	15	4,022	179	0.0242	0.0011
1.150	410	20	6,195	302	0.0343	0.0017
1.050	501	22	5,043	222	0.0263	0.0012
0.950	708	27	5,864	223	0.0277	0.0010
0.850	1,000	32	6,458	213	0.0288	0.0009
0.750	1,217	34	5,439	152	0.0207	0.0006
0.650	1,696	40	6,496	153	0.0221	0.0005
0.550	2,370	49	7,425	153	0.0214	0.0004
0.450	3,657	60	9,448	155	0.0222	0.0004
0.350	6,484	80	13,213	163	0.0236	0.0003
0.250	14,960	122	21,898	178	0.0265	0.0002
0.150	45,076	212	46,749	220	0.0290	0.0001
0.050	123,575	352	114,495	326	0.0710	0.0002

Table 23. Experimental energy spectrum

Position: vertical 15 cm
radial 5 cm

Gamma energy (Mev)	Corrected count rate (cpm)	Standard deviation (cpm)	Photon rate (photons per min)	Standard deviation (photons per min)	Dose rate (mr/hr)	Standard deviation (mr/hr)
1.350	24,992	158	552,920	3,490	3.480	0.022
1.250	55,716	236	998,968	4,230	6.000	0.025
1.150	76,734	277	1,071,081	3,690	5.660	0.020
1.050	84,644	291	698,266	2,400	3.630	0.012
0.950	92,338	304	462,907	1,524	2.170	0.007
0.850	121,397	348	607,269	1,740	2.628	0.008
0.750	127,122	356	343,575	961	1.310	0.004
0.650	130,814	362	190,901	528	0.609	0.002
0.550	149,163	386	209,138	542	0.600	0.001
0.450	193,234	440	301,166	686	0.708	0.002
0.350	294,476	543	436,691	790	0.777	0.001
0.250	568,083	754	711,546	943	0.856	0.001
0.150	1,210,425	1,101	1,175,775	1,023	0.698	0.001
0.050	2,741,012	1,657	2,397,434	1,448	1.486	0.001

Table 24. Experimental energy spectrum

Position: vertical 15 cm
radial 7 cm

Gamma energy (Mev)	Corrected count rate (cpm)	Standard deviation (cpm)	Photon rate (photons per min)	Standard deviation (photons per min)	Dose rate (mr/hr)	Standard deviation (mr/hr)
1.350	24,998	158	553,053	3,490	3.490	0.022
1.250	43,465	208	735,462	3,510	4.420	0.021
1.150	64,312	254	1,056,091	4,170	5.850	0.023
1.050	67,386	260	445,279	1,720	2.320	0.009
0.950	76,737	277	369,020	1,333	1.735	0.006
0.850	100,893	316	497,568	1,573	2.150	0.007
0.750	105,639	325	282,145	868	1.079	0.003
0.650	111,733	334	177,860	533	0.604	0.002
0.550	129,338	360	201,225	560	0.578	0.001
0.450	171,832	415	290,175	701	0.682	0.002
0.350	266,944	517	430,806	833	0.767	0.001
0.250	531,047	730	691,372	950	0.832	0.001
0.150	1,161,033	1,079	1,100,705	1,022	0.682	0.001
0.050	2,371,587	1,541	2,058,097	1,338	1.277	0.001

Table 25. Experimental energy spectrum

Position: vertical 15 cm
radial 10 cm

Gamma energy (Mev)	Corrected count rate (cpm)	Standard deviation (cpm)	Photon rate (photons per min)	Standard deviation (photons per min)	Dose rate (mr/hr)	Standard deviation (mr/hr)
1.350	20,630	144	456,416	3,133	2.880	0.020
1.250	31,308	177	508,839	2,875	3.055	0.017
1.150	43,454	220	653,992	2,965	3.620	0.016
1.050	50,537	225	389,750	1,735	2.030	0.009
0.950	59,105	243	329,369	1,354	1.549	0.006
0.850	76,526	277	387,853	1,403	1.675	0.006
0.750	81,298	285	231,549	812	0.895	0.003
0.650	88,967	298	171,471	574	0.583	0.002
0.550	105,547	325	133,469	530	0.542	0.002
0.450	142,663	378	259,744	688	0.611	0.002
0.350	228,529	478	388,106	811	0.691	0.001
0.250	466,603	684	622,952	913	0.750	0.001
0.150	1,061,866	1,030	1,024,083	993	0.635	0.001
0.050	2,182,429	1,478	1,909,107	1,293	1.183	0.001

Table 26. Experimental energy spectrum

Position: vertical 15 cm
radial 15 cm

Gamma energy (Mev)	Corrected count rate (cpm)	Standard deviation (cpm)	Photon rate (photons per min)	Standard deviation (photons per min)	Dose rate (mr/hr)	Standard deviation (mr/hr)
1.350	13,642	117	301,814	2,585	1.900	0.016
1.250	18,340	135	285,677	2,100	1.713	0.013
1.150	30,130	174	412,162	2,383	2.280	0.013
1.050	31,571	178	246,204	1,386	1.283	0.007
0.950	38,148	195	227,409	1,163	1.070	0.005
0.850	50,135	224	267,228	1,193	1.155	0.005
0.750	53,787	232	163,478	705	0.622	0.003
0.650	60,838	247	134,587	546	0.457	0.002
0.550	74,343	273	151,000	555	0.434	0.002
0.450	102,450	320	200,794	626	0.472	0.001
0.350	171,700	414	308,724	745	0.550	0.001
0.250	363,637	603	500,272	829	0.602	0.001
0.150	869,958	928	855,490	912	0.530	0.001
0.050	1,895,730	1,377	1,684,499	1,224	1.043	0.001

Table 27. Experimental energy spectrum

Position: vertical 15 cm
radial 25 cm

Gamma energy (Mev)	Corrected count rate (cpm)	Standard deviation (cpm)	Photon rate (photons per min)	Standard deviation (photons per min)	Dose rate (mr/hr)	Standard deviation (mr/hr)
1.350	5,178	72	114,558	1,593	0.723	0.010
1.250	6,328	80	86,237	1,360	0.548	0.008
1.150	11,033	105	148,233	1,410	0.823	0.008
1.050	12,059	110	99,017	904	0.516	0.005
0.950	15,314	124	101,595	822	0.478	0.004
0.850	19,962	141	109,769	775	0.475	0.003
0.750	22,796	151	81,603	540	0.312	0.002
0.650	26,778	164	71,008	434	0.241	0.001
0.550	34,674	186	84,487	453	0.243	0.001
0.450	50,360	224	112,166	498	0.264	0.001
0.350	86,537	294	164,861	561	0.294	0.001
0.250	191,535	438	271,783	622	0.327	0.001
0.150	506,342	712	511,240	719	0.317	0.001
0.050	1,204,876	1,099	1,092,188	1,000	0.677	0.001

Table 28. Experimental energy spectrum

Position: vertical 15 cm
radial 35 cm

Gamma energy (Mev)	Corrected count rate (cpm)	Standard deviation (cpm)	Photon rate (photons per min)	Standard deviation (photons per min)	Dose rate (mr/hr)	Standard deviation (mr/hr)
1.350	1,875	43	41,482	950	0.262	0.006
1.250	2,434	49	37,398	752	0.225	0.004
1.150	4,243	65	59,480	912	0.330	0.005
1.050	4,740	69	41,368	601	0.215	0.003
0.950	6,294	79	45,664	572	0.215	0.003
0.850	8,235	91	47,323	523	0.205	0.002
0.750	9,701	99	37,822	390	0.144	0.001
0.650	12,162	110	37,992	344	0.129	0.001
0.550	16,244	128	44,312	349	0.128	0.001
0.450	24,227	156	57,735	372	0.136	0.001
0.350	42,962	208	85,203	413	0.152	0.001
0.250	96,795	312	139,663	450	0.168	0.001
0.150	271,295	521	277,601	532	0.172	0.001
0.050	685,247	829	627,705	759	0.389	0.001

Table 29. Experimental energy spectrum

Position: vertical 15 cm
radial 55 cm

Gamma energy (Mev)	Corrected count rate (cpm)	Standard deviation (cpm)	Photon rate (photons per min)	Standard deviation (photons per min)	Dose rate (mr/hr)	Standard deviation (mr/hr)
1.350	307	17	6,792	376	0.0430	0.0024
1.250	433	21	6,860	332	0.0413	0.0020
1.150	710	27	9,771	371	0.0541	0.0020
1.050	912	30	9,114	300	0.0473	0.0015
0.950	1,113	33	7,708	229	0.0363	0.0011
0.850	1,609	40	10,272	256	0.0445	0.0011
0.750	1,997	45	8,971	210	0.0342	0.0008
0.650	2,632	51	9,439	183	0.0371	0.0006
0.550	3,821	62	12,100	197	0.0350	0.0006
0.450	5,585	75	13,901	187	0.0327	0.0004
0.350	10,363	102	21,324	210	0.0380	0.0003
0.250	23,501	153	34,333	223	0.0413	0.0003
0.150	69,257	263	71,586	272	0.0444	0.0002
0.050	184,721	430	170,585	397	0.1055	0.0002

Table 30. Experimental energy spectrum

Position: vertical 0 cm
radial 20 cm

Gamma energy (Mev)	Corrected count rate (cpm)	Standard deviation (cpm)	Photon rate (photons per min)	Standard deviation (photons per min)	Dose rate (mr/hr)	Standard deviation (mr/hr)
1.350	19,115	138	422,893	3,050	2.665	0.019
1.250	25,213	159	389,849	2,460	2.345	0.015
1.150	40,898	202	554,033	2,735	3.070	0.015
1.050	41,370	204	306,243	1,507	1.593	0.008
0.950	51,177	226	309,367	1,370	1.458	0.006
0.850	65,237	255	333,247	1,303	1.440	0.006
0.750	70,878	266	215,645	808	0.824	0.003
0.650	79,816	282	173,678	614	0.591	0.002
0.550	96,549	310	191,163	615	0.550	0.002
0.450	131,280	362	250,381	691	0.588	0.002
0.350	211,838	460	367,409	796	0.654	0.001
0.250	451,157	672	615,548	916	0.761	0.001
0.150	1,045,125	1,023	1,018,671	999	0.631	0.001
0.050	2,223,265	1,492	1,992,817	1,336	1.236	0.001

Table 31. Experimental energy spectrum

Position: vertical 0 cm
radial 35 cm

Gamma energy (Mev)	Corrected count rate (cpm)	Standard deviation (cpm)	Photon rate (photons per min)	Standard deviation (photons per min)	Dose rate (mr/hr)	Standard deviation (mr/hr)
1.350	3,188	56	70,531	1,239	0.442	0.008
1.250	3,806	62	56,430	919	0.339	0.006
1.150	6,688	82	92,911	1,139	0.515	0.006
1.050	7,314	86	61,734	727	0.322	0.004
0.950	9,500	98	65,947	681	0.310	0.003
0.850	13,320	115	82,174	708	0.356	0.003
0.750	14,110	119	46,663	393	0.178	0.002
0.650	17,647	133	51,017	385	0.173	0.001
0.550	22,840	151	57,700	382	0.166	0.001
0.450	34,009	185	78,650	427	0.195	0.001
0.350	59,394	244	115,655	475	0.206	0.001
0.250	135,025	368	194,315	530	0.234	0.001
0.150	367,981	607	374,735	618	0.232	0.001
0.050	909,056	954	829,620	871	0.514	0.001

Table 32. Experimental energy spectrum

Position: vertical 0 cm
radial 55 cm

Gamma energy (Mev)	Corrected count rate (cpm)	Standard deviation (cpm)	Photon rate (photons per min)	Standard deviation (photons per min)	Dose rate (mr/hr)	Standard deviation (mr/hr)
1.350	402	20	8,894	442	0.0562	0.0028
1.250	506	22	7,677	334	0.0462	0.0020
1.150	878	30	12,225	418	0.0677	0.0023
1.050	1,130	34	11,773	354	0.0613	0.0018
0.950	1,485	39	11,213	294	0.0528	0.0014
0.850	2,053	45	12,867	283	0.0556	0.0012
0.750	2,387	49	9,588	197	0.0366	0.0008
0.650	3,233	57	11,471	202	0.0390	0.0007
0.550	4,517	67	13,700	203	0.0394	0.0006
0.450	7,003	84	17,928	215	0.0422	0.0005
0.350	12,455	112	25,374	228	0.0452	0.0004
0.250	29,024	170	42,567	250	0.0513	0.0003
0.150	85,535	292	88,499	302	0.0548	0.0002
0.050	225,572	475	208,181	438	0.1290	0.0003

Table 33. Experimental energy spectrum without the dust

Position: vertical 30 cm
radial 0 cm

Gamma energy (Mev)	Corrected count rate (cpm)	Standard deviation (cpm)	Photon rate (photons per min)	Standard deviation (photons per min)	Dose rate (mr/hr)	Standard deviation (mr/hr)
1.350	8,009	90	177,190	1,993	1.118	0.013
1.250	9,717	99	145,140	1,458	0.873	0.009
1.150	14,353	120	181,247	1,515	1.003	0.009
1.050	15,161	123	112,466	913	0.585	0.005
0.950	20,641	144	145,000	1,011	0.682	0.005
0.850	25,370	159	130,802	819	0.566	0.004
0.750	28,648	169	96,165	517	0.367	0.002
0.650	33,971	184	88,884	480	0.302	0.002
0.550	43,730	209	104,975	502	0.302	0.001
0.450	62,785	250	137,417	547	0.323	0.001
0.350	105,595	325	197,394	608	0.352	0.001
0.250	230,499	480	323,907	673	0.390	0.001
0.150	594,432	765	553,749	723	0.343	0.001
0.050	1,244,965	1,116	1,086,929	970	0.673	0.001

Table 3h. Experimental energy spectrum without the duct

Position: vertical 30 cm
radial 5 cm

Gamma energy (Mev)	Corrected count rate (cpm)	Standard deviation (cpm)	Photon rate (photons per min)	Standard deviation (photons per min)	Dose rate (mr/hr)	Standard deviation (mr/hr)
1.350	6,963	83	154,049	1,838	0.972	0.012
1.250	8,563	92	128,645	1,353	0.774	0.008
1.150	12,698	113	161,185	1,434	0.894	0.008
1.050	13,702	117	105,511	901	0.549	0.005
0.950	18,452	136	129,535	955	0.610	0.004
0.850	22,747	151	117,799	782	0.509	0.003
0.750	25,845	161	88,191	550	0.337	0.002
0.650	30,893	176	82,876	472	0.282	0.002
0.550	40,210	200	99,238	493	0.286	0.001
0.450	57,977	241	128,803	535	0.303	0.001
0.350	98,692	314	186,806	595	0.332	0.001
0.250	216,268	466	305,370	658	0.368	0.001
0.150	553,743	744	555,429	746	0.344	0.001
0.050	1,198,858	1,096	1,072,896	982	0.665	0.001

Table 35. Experimental energy spectrum without the duct

Position: vertical 30 cm
radial 10 cm

Gamma energy (Mev)	Corrected count rate (cpm)	Standard deviation (cpm)	Photon rate (photons per min)	Standard deviation (photons per min)	Dose rate (mr/hr)	Standard deviation (mr/hr)
1.350	5,573	75	123,296	1,656	0.779	0.010
1.250	7,091	84	108,065	1,235	0.650	0.007
1.150	10,292	101	129,730	1,272	0.718	0.007
1.050	11,272	106	88,227	829	0.459	0.004
0.950	15,302	124	109,286	885	0.514	0.004
0.850	18,838	137	98,193	714	0.424	0.003
0.750	21,511	147	74,496	509	0.288	0.002
0.650	25,647	160	68,959	431	0.234	0.001
0.550	33,791	184	85,019	463	0.244	0.001
0.450	49,493	222	112,502	505	0.264	0.001
0.350	85,101	292	163,303	560	0.291	0.001
0.250	187,432	433	266,113	615	0.320	0.001
0.150	492,312	702	496,644	708	0.308	0.001
0.050	1,082,613	1,041	972,718	935	0.603	0.001

Table 36. Experimental energy spectrum without the duct

Position: vertical 30 cm
radial 15 cm

Gamma energy (Mev)	Corrected count rate (cpm)	Standard deviation (cpm)	Photon rate (photons per min)	Standard deviation (photons per min)	Dose rate (mr/hr)	Standard deviation (mr/hr)
1.350	4,205	65	93,031	1,435	0.588	0.009
1.250	5,165	72	77,548	1,059	0.466	0.006
1.150	7,741	88	98,898	1,125	0.549	0.006
1.050	8,262	91	62,909	693	0.327	0.004
0.950	11,362	106	81,678	762	0.384	0.004
0.850	13,983	118	73,098	617	0.316	0.003
0.750	16,390	128	59,978	469	0.229	0.002
0.650	20,110	142	58,744	415	0.200	0.001
0.550	27,062	164	72,512	439	0.209	0.001
0.450	39,761	199	92,843	465	0.218	0.001
0.350	69,405	264	135,548	515	0.241	0.001
0.250	153,964	392	220,181	560	0.265	0.001
0.150	415,989	645	422,347	654	0.262	0.001
0.050	928,927	965	838,146	870	0.519	0.001

Table 37. Experimental energy spectrum without the duct

Position: vertical 30 cm
radial 25 cm

Gamma energy (Mev)	Corrected count rate (cpm)	Standard deviation (cpm)	Photon rate (photons per min)	Standard deviation (photons per min)	Dose rate (mr/hr)	Standard deviation (mr/hr)
1.350	1,926	44	42,611	972	0.269	0.006
1.250	2,563	50	39,763	776	0.239	0.004
1.150	3,783	62	43,399	793	0.268	0.004
1.050	4,276	65	35,376	538	0.184	0.002
0.950	5,980	77	45,282	583	0.213	0.002
0.850	7,423	86	40,394	468	0.175	0.002
0.750	8,835	94	36,030	362	0.130	0.001
0.650	11,000	105	33,777	322	0.115	0.001
0.550	15,113	123	42,419	345	0.122	0.001
0.450	22,983	152	56,291	371	0.133	0.001
0.350	40,978	202	82,248	405	0.146	0.001
0.250	93,657	306	136,139	445	0.164	0.001
0.150	263,093	513	269,814	527	0.167	0.001
0.050	614,128	784	558,792	714	0.346	0.001

Table XX. Experimental energy spectrum without the duct

Position: vertical 30 cm
radial 40 cm

Gamma energy (Mev)	Corrected count rate (cpm)	Standard deviation (cpm)	Photon rate (photons per min)	Standard deviation (photons per min)	Dose rate (mr/hr)	Standard deviation (mr/hr)
1.350	685	26	15,155	574	0.096	0.004
1.250	857	29	13,011	427	0.078	0.003
1.150	1,060	35	15,988	444	0.089	0.002
1.050	1,501	39	13,199	343	0.069	0.002
0.950	2,163	46	17,326	368	0.082	0.002
0.850	2,741	52	15,802	311	0.068	0.001
0.750	3,375	58	14,398	247	0.055	0.001
0.650	4,357	66	14,835	224	0.050	0.001
0.550	6,137	78	18,463	235	0.055	0.001
0.450	9,751	99	25,345	258	0.060	0.001
0.350	17,318	131	35,412	268	0.063	0.001
0.250	40,149	200	58,893	294	0.071	0.001
0.150	117,206	342	121,122	354	0.075	0.001
0.050	281,783	531	257,810	486	0.160	0.001

Table 39. Experimental energy spectrum outside the tank

Position: vertical 30 cm
radial 0 cm

Gamma energy (Mev)	Corrected count rate (cpm)	Standard deviation (cpm)	Photon rate (photons per min)	Standard deviation (photons per min)	Dose rate (mr/hr)	Standard deviation (mr/hr)
1.350	19,521	140	431,881	3,096	2.720	0.019
1.250	21,371	146	304,000	2,095	1.829	0.013
1.150	32,482	180	408,732	2,265	2.270	0.013
1.050	30,396	174	178,304	1,020	0.928	0.005
0.950	42,235	206	282,226	1,375	1.328	0.006
0.850	49,104	222	222,853	1,010	0.964	0.004
0.750	49,330	222	105,785	476	0.404	0.002
0.650	53,099	230	80,521	349	0.273	0.001
0.550	60,902	247	88,606	360	0.255	0.001
0.450	75,894	276	111,094	404	0.261	0.001
0.350	109,179	330	155,570	468	0.277	0.001
0.250	202,187	450	285,220	546	0.295	0.001
0.150	403,973	636	365,070	575	0.226	0.001
0.050	667,280	817	544,411	667	0.337	0.001

Table 40. Experimental energy spectrum outside the tank

Position: vertical 30 cm
radial 6 cm

Gamma energy (Mev)	Corrected count rate (cpm)	Standard deviation (cpm)	Photon rate (photons per min)	Standard deviation (photons per min)	Dose rate (mr/hr)	Standard deviation (mr/hr)
1.350	12,189	110	268,341	2,430	1.693	0.015
1.250	13,739	117	193,774	1,680	1.195	0.010
1.150	20,539	143	257,588	1,800	1.426	0.010
1.050	19,064	138	109,287	792	0.570	0.004
0.950	26,274	159	172,209	1,043	0.810	0.005
0.850	31,101	176	144,620	818	0.625	0.004
0.750	32,444	180	81,571	453	0.312	0.002
0.650	36,067	190	68,025	359	0.231	0.001
0.550	42,703	205	75,119	360	0.216	0.001
0.450	55,178	235	93,130	397	0.219	0.001
0.350	83,284	288	131,030	454	0.233	0.001
0.250	162,475	403	208,170	517	0.250	0.001
0.150	355,123	596	334,857	562	0.208	0.001
0.050	618,316	786	521,033	663	0.323	0.001

Table 41. Experimental energy spectrum outside the tank

Position: vertical 30 cm
radial 11 cm

Gamma energy (Mev)	Corrected count rate (cpm)	Standard deviation (cpm)	Photon rate (photons per min)	Standard deviation (photons per min)	Dose rate (mr/hr)	Standard deviation (mr/hr)
1.350	6,300	79	139,381	1,747	0.880	0.011
1.250	7,439	86	109,763	1,234	0.660	0.007
1.150	11,280	106	144,033	1,352	0.799	0.007
1.050	11,301	106	77,399	726	0.402	0.004
0.950	15,572	125	108,090	867	0.509	0.004
0.850	18,576	136	90,421	662	0.391	0.003
0.750	20,267	142	60,249	422	0.230	0.002
0.650	23,494	153	54,793	357	0.186	0.001
0.550	29,159	171	62,519	366	0.180	0.001
0.450	39,833	199	78,821	394	0.185	0.001
0.350	63,599	252	110,830	438	0.197	0.001
0.250	129,262	360	173,593	483	0.209	0.001
0.150	305,516	553	297,509	539	0.184	0.001
0.050	558,117	747	401,683	644	0.298	0.001

Table 42. Experimental energy spectrum outside the tank

Position: vertical 30 cm
radial 16 cm

Gamma energy (Mev)	Corrected count rate (cpm)	Standard deviation (cpm)	Photon rate (photons per min)	Standard deviation (photons per min)	Dose rate (mr/hr)	Standard deviation (mr/hr)
1.350	4,650	68	102,876	1,503	0.650	0.009
1.250	5,324	73	77,419	1,047	0.465	0.006
1.150	8,243	91	105,946	1,170	0.587	0.006
1.050	8,559	92	62,736	674	0.326	0.004
0.950	11,726	108	82,708	762	0.389	0.004
0.850	14,286	119	72,201	603	0.312	0.003
0.750	15,941	126	51,842	409	0.198	0.002
0.650	18,281	135	43,537	321	0.148	0.001
0.550	23,804	154	56,063	362	0.161	0.001
0.450	33,402	183	70,794	388	0.162	0.001
0.350	53,238	230	94,970	410	0.169	0.001
0.250	108,813	330	147,470	447	0.178	0.001
0.150	263,717	514	258,677	504	0.160	0.001
0.050	490,474	701	425,939	601	0.264	0.001

Table 43. Experimental energy spectrum outside the tank

Position: vertical 30 cm
radial 31 cm

Gamma energy (Mev)	Corrected count rate (cpm)	Standard deviation (cpm)	Photon rate (photons per min)	Standard deviation (photons per min)	Dose rate (mr/hr)	Standard deviation (mr/hr)
1.350	1,915	44	42,367	973	0.268	0.006
1.250	2,163	46	31,247	660	0.188	0.004
1.150	3,431	59	45,676	725	0.253	0.004
1.050	4,017	63	36,760	545	0.151	0.003
0.950	5,166	72	35,764	498	0.168	0.002
0.850	6,680	82	36,984	454	0.156	0.002
0.750	7,676	88	27,941	320	0.107	0.001
0.650	9,242	96	25,983	271	0.088	0.001
0.550	12,173	110	31,175	281	0.090	0.001
0.450	17,415	132	38,942	295	0.092	0.001
0.350	28,967	170	54,182	317	0.096	0.001
0.250	59,330	245	82,665	338	0.100	0.001
0.150	150,504	388	149,501	385	0.093	0.001
0.050	284,804	533	249,415	467	0.155	0.001

Table 44. Experimental and calculated data without the duct

Vertical distance from source (cm)	Radial distance from duct (cm)	Dose rate experimental (mr/hr)	Standard deviation (mr/hr)	Dose rate calculated (mr/hr)
30	0	7.879	0.020	8.43
30	5	7.225	0.018	8.08
30	10	6.092	0.016	7.49
30	15	4.772	0.014	6.13
30	25	2.671	0.009	3.73
30	40	1.071	0.007	1.44

Table 45. Experimental data measured out of the water

Depth of source (cm)	Radial distance from duct (cm)	Dose rate (mr/hr)	Standard deviation (mr/hr)	Normalised
30.5	0.0	12.367	0.028	1.000
30.5	1.0	12.134	0.028	0.934
30.5	4.5	10.710	0.024	0.866
30.5	6.0	8.311	0.022	0.672
30.5	11.0	5.310	0.016	0.429
30.5	16.0	4.169	0.016	0.337
30.5	31.0	2.035	0.010	0.165